



OPEN ACCESS

EDITED BY

Na'il Saleh,
United Arab Emirates University, United
Arab Emirates

REVIEWED BY

Sayed Ashique Ahmed,
Indian Institute of Science (IISc), India
Chi Hu,
China Pharmaceutical University, China

*CORRESPONDENCE

Hai-Ping Yang,
oyhp@hospital.cqmu.edu.cn
Qiu Li,
liqiu809@126.com

†These authors have contributed equally
to this work and share first authorship

SPECIALTY SECTION

This article was submitted to
Supramolecular Chemistry,
a section of the journal
Frontiers in Chemistry

RECEIVED 21 June 2022

ACCEPTED 11 July 2022

PUBLISHED 24 August 2022

CITATION

Xiao H, Yang X, Yang L, Yang D, Luo Y,
Yang H-P, Tao Z, Xiao X and Li Q (2022),
Cucurbit [8] uril-based supramolecular
fluorescent biomaterials for cytotoxicity
and imaging studies of kidney cells.
Front. Chem. 10:974607.
doi: 10.3389/fchem.2022.974607

COPYRIGHT

© 2022 Xiao, Yang, Yang, Yang, Luo,
Yang, Tao, Xiao and Li. This is an open-
access article distributed under the
terms of the [Creative Commons
Attribution License \(CC BY\)](https://creativecommons.org/licenses/by/4.0/). The use,
distribution or reproduction in other
forums is permitted, provided the
original author(s) and the copyright
owner(s) are credited and that the
original publication in this journal is
cited, in accordance with accepted
academic practice. No use, distribution
or reproduction is permitted which does
not comply with these terms.

Cucurbit [8] uril-based supramolecular fluorescent biomaterials for cytotoxicity and imaging studies of kidney cells

Han Xiao^{1†}, Xia Yang^{1†}, Li Yang¹, Dan Yang², Yang Luo²,
Hai-Ping Yang^{1*}, Zhu Tao², Xin Xiao² and Qiu Li^{1*}

¹Department of Nephrology, Children's Hospital of Chongqing Medical University, National Clinical Research Center for Child Health and Disorders, Ministry of Education Key Laboratory of Child Development and Disorders, Chongqing Key Laboratory of Pediatrics, Chongqing, China, ²Key Laboratory of Macrocyclic and Supramolecular Chemistry of Guizhou Province, Institute of Applied Chemistry, Guizhou University, Guiyang, China

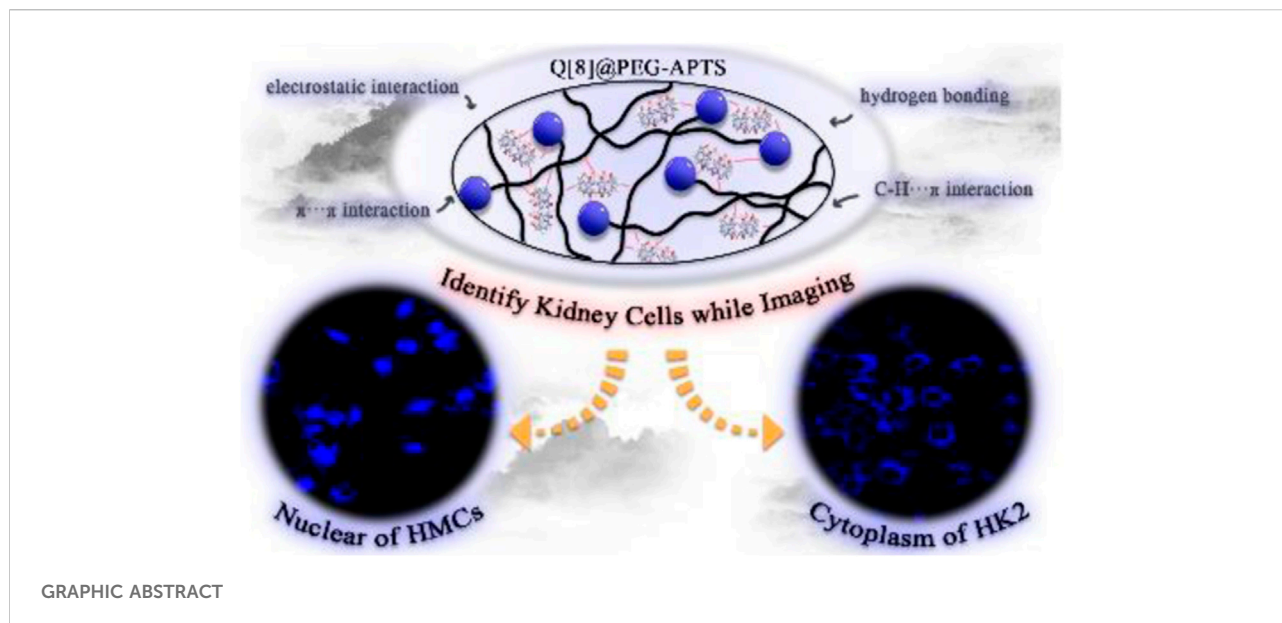
An accurate diagnosis of acute kidney injury (AKI) at the early stage is critical to not only allow preventative treatments in time but also forecast probable medication toxicity for preventing AKI from starting and progressing to severe kidney damage and death. Therefore, supramolecular fluorescent biomaterials based on Q [8] and PEG-APTS have been prepared herein. This study has found that the unique properties of outer surface methine and the positive density of Q [8] can form a stable assembly with PEG-APTS, and has provided the possibility for the faster crossing of the glomerular filtration barrier to enter into the resident cells of the kidney. In addition to the excellent fluorescence properties, the as-synthesized biomaterial Q [8]@PEG-APTS has possessed significantly low biological toxicity. Most importantly, the accumulation of Q [8]@PEG-APTS in large amounts in cytoplasm and nucleus of HK2 and HMCs cells, respectively, within 24 h enabled distinguishing kidney cells when diagnosing and providing some foundation for early AKI.

KEYWORDS

acute kidney injury, supramolecular fluorescent biomaterials, excellent fluorescence properties, low biological toxicity, macrocyclic host

Introduction

Acute kidney injury (AKI) is broadly defined as the sudden loss of kidney function and has become a worldwide health problem to expedite morbidity and mortality (Chawla et al., 2014; Kellum et al., 2021). Several conditions can precipitate AKI (Goldstein et al., 2016; Sato et al., 2017; Kao et al., 2019; Peerapornratana et al., 2019), such as sepsis, hypotension, organ failure, kidney stone, and abusing medications. Moreover, variegated medications, such as cisplatin (anticancer drug), acyclovir (antiviral agent), aminoglycoside (antibiotic), and others, have been proven to cause severe nephrotoxicity and AKI in people (Pazhayattil and Shirali, 2014). The accurate

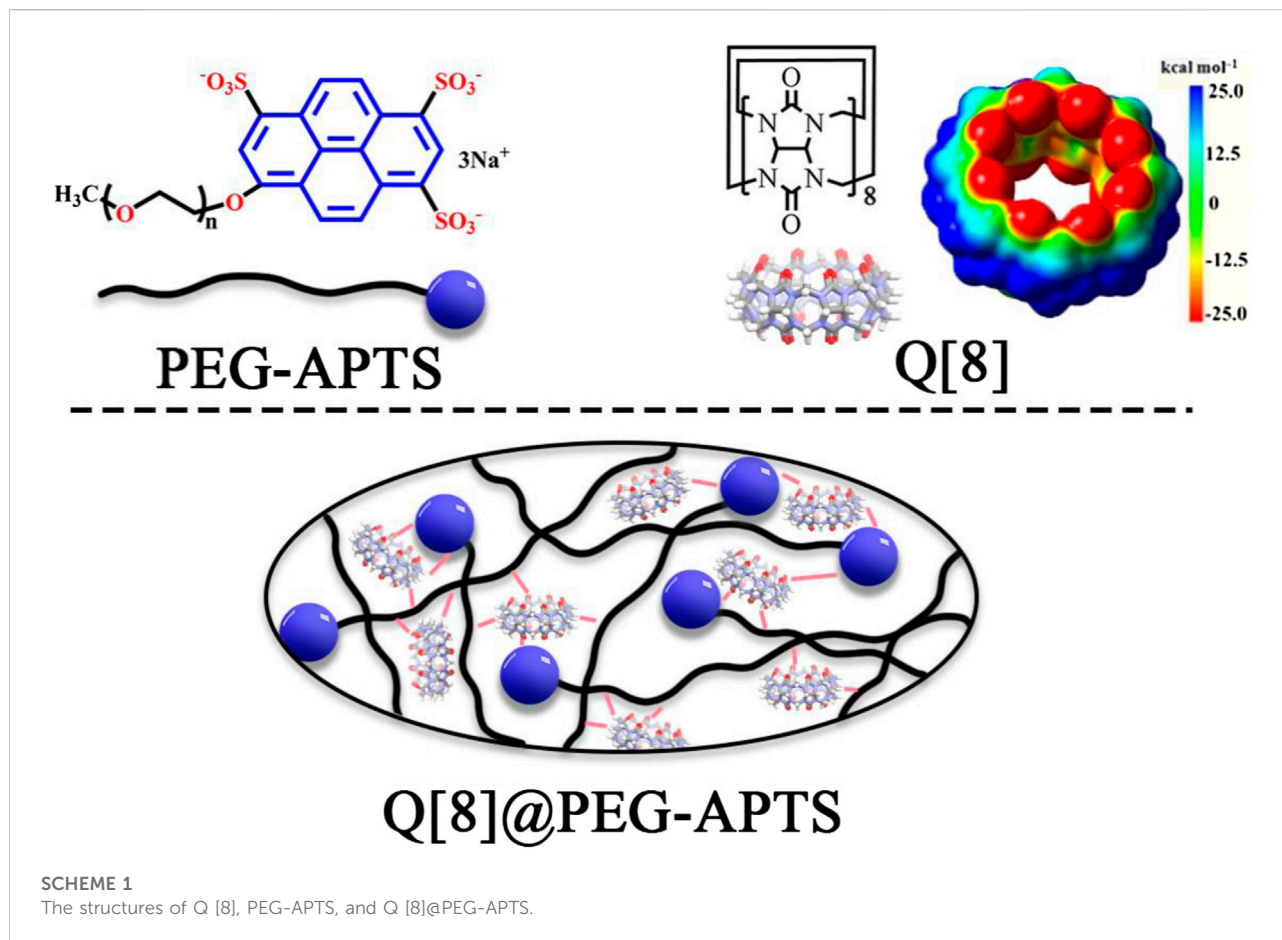


diagnosis of AKI at an early stage is critical in not only offering preventative treatments in time, but also forecasting probable medication toxicity for preventing AKI from starting, spreading, and propagating into severe kidney damage and death (Basile et al., 2016). Traditional imaging methods, (Lerman et al., 1999; Kobayashi et al., 2002; Fisch et al., 2016) such as computed tomography, magnetic resonance imaging, and ultrasound imaging, help for AIK diagnosis, primarily through noninvasive *in vivo* imaging of adjustments in kidney anatomy and histology, yet, the lack of capacity to detect AKI-associated biomarkers at the molecular level has hampered the capacity to discern AKI at an early stage. Recently, fluorescence imaging (Cui et al., 2020; Moore et al., 2021; Wu et al., 2021) has shown potential for AKI diagnosis because of its high sensitivity, low cost, and simplicity to use. It has the potential to offer valuable information on kidney anatomic changes, decreased renal perfusion, and aberrant biomolecule levels in the kidney, allowing noninvasive and real-time diagnosis of kidney dysfunction in patients.

In recent years, researchers have become much more interested in supramolecular self-assemblies incorporating fluorescence for cell imaging (Palivan et al., 2016; Li et al., 2018). Few non-fluorescent organic dyes can be transformed into fluorescent to emit diverse fluorescence emissions in supramolecular self-assemblies *via* either host-guest complexation or triggering the aggregation-induced emission (AIE) effect (Mei et al., 2015). At high concentrations, supramolecular self-assemblies may also inhibit dye aggregation and aggregation-induced quenching (ACQ). Therefore, a large number of supramolecular self-assembled materials have been applied in cellular imaging or other smart materials. Cucurbit [n]uril [Q (n)s or CB (n)s, $n = 5-8, 10,$

13–15], is usually used for designing supramolecular assemblies (Kim et al., 2000; Cheng et al., 2013; Chen et al., 2021; Liu et al., 2021; Luo et al., 2022a; Zhang et al., 2022a; Luo et al., 2022b; Zhang et al., 2022b; Zhang et al., 2022c). Cucurbit [n]urils are classical macrocyclic hosts formed by acid-catalyzed condensation of glycoluril and formaldehyde (Figure 2) having cavity sizes within 2.4–11.0 Å and a common depth of 9.1 Å. From the structural point of view, the rigid cavity of Q [n] derives the classical Q [n]-based host-guest chemistry, the rich carbonyl oxygen of its portal yields the Q [n]-based coordination chemistry, and positively density outer surface of the Q [n] rich in methane breeds the novel outer surface interaction of Q [n] (Ni et al., 2014). Therefore, compared with other macrocycles (Liu Z. et al., 2017; Murray et al., 2017), Q [n]s distinguish themselves *via* the excellent ability to form inclusion complexes with various guest molecules through host-guest, coordination, and out surface interactions (Assaf and Nau, 2015; Barrow et al., 2015; Liu J. et al., 2017; Jia et al., 2019; Lin et al., 2020; Yang et al., 2021; Zhang et al., 2021; Wang et al., 2022).

Herein, a polymer chain (i.e., PEG-APTS, Scheme 1 for structure, Supplementary Scheme S2 for synthetic route) was designed by utilizing polyethylene glycol and sodium pyrene sulfonate. Q [8] was selected as the supramolecular host because of its excellent cavity properties among other common cucurbit [n]urils. Subsequently, the supramolecular fluorescent biomaterial Q [8]@PEG-APTS, synthesized by employing the outer surface interaction within PEG-APTS and Q [8], was demonstrated to possess a stable and uniform structure and good fluorescence properties. Most importantly, the positive density on the outer surface of Q [8] could neutralize the negative charge of sulfonate on PEG-APTS, enabling the rapid infiltration of Q [8]@PEG-APTS through the glomerular filtration



barrier and entering the kidney resident cells. In addition, the as-synthesized biomaterial also possessed low biotoxicity and is capable of massive intracellular accumulation within 24 h. Moreover, Q [8]@PEG-APTS was found to track specifically different organelles in different cells, such as the selective accumulation in the cytoplasm in HK2 cells, specifically in the perinuclear of HMCs cells, which might be helpful to identify diverse cell types during tracing living cells in the kidney. This work provides an ideal cellular imaging supramolecular fluorescent biomaterial for the early-stage diagnosis of AKI and provides a theoretical basis for the potential application of Q [n]-based fluorescent biomaterials in kidney research and therapy.

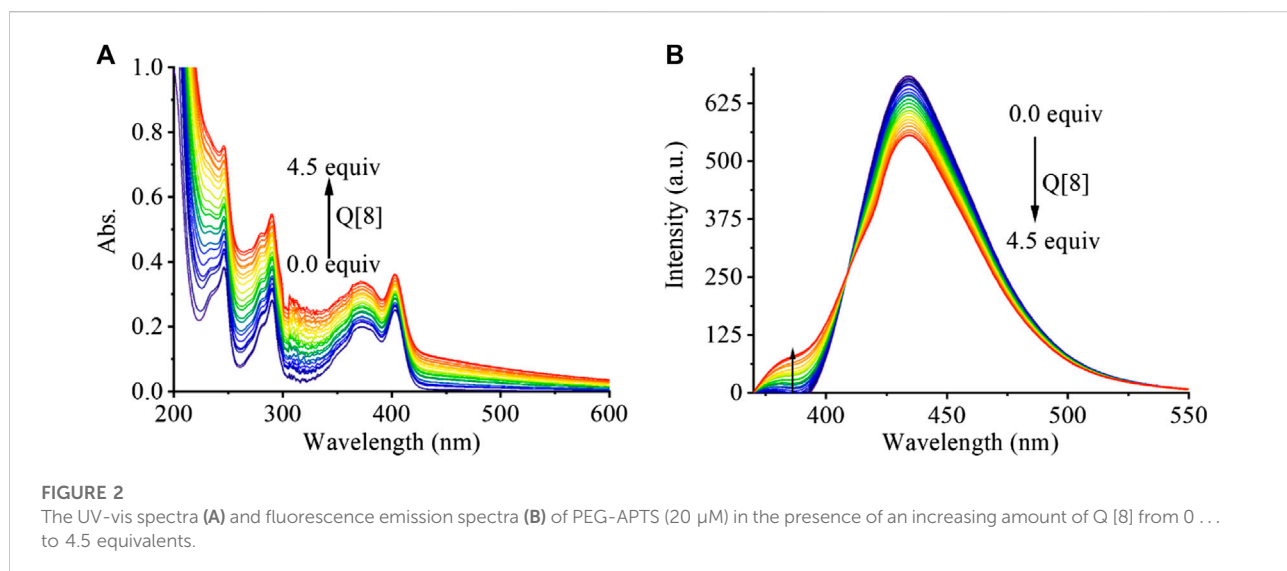
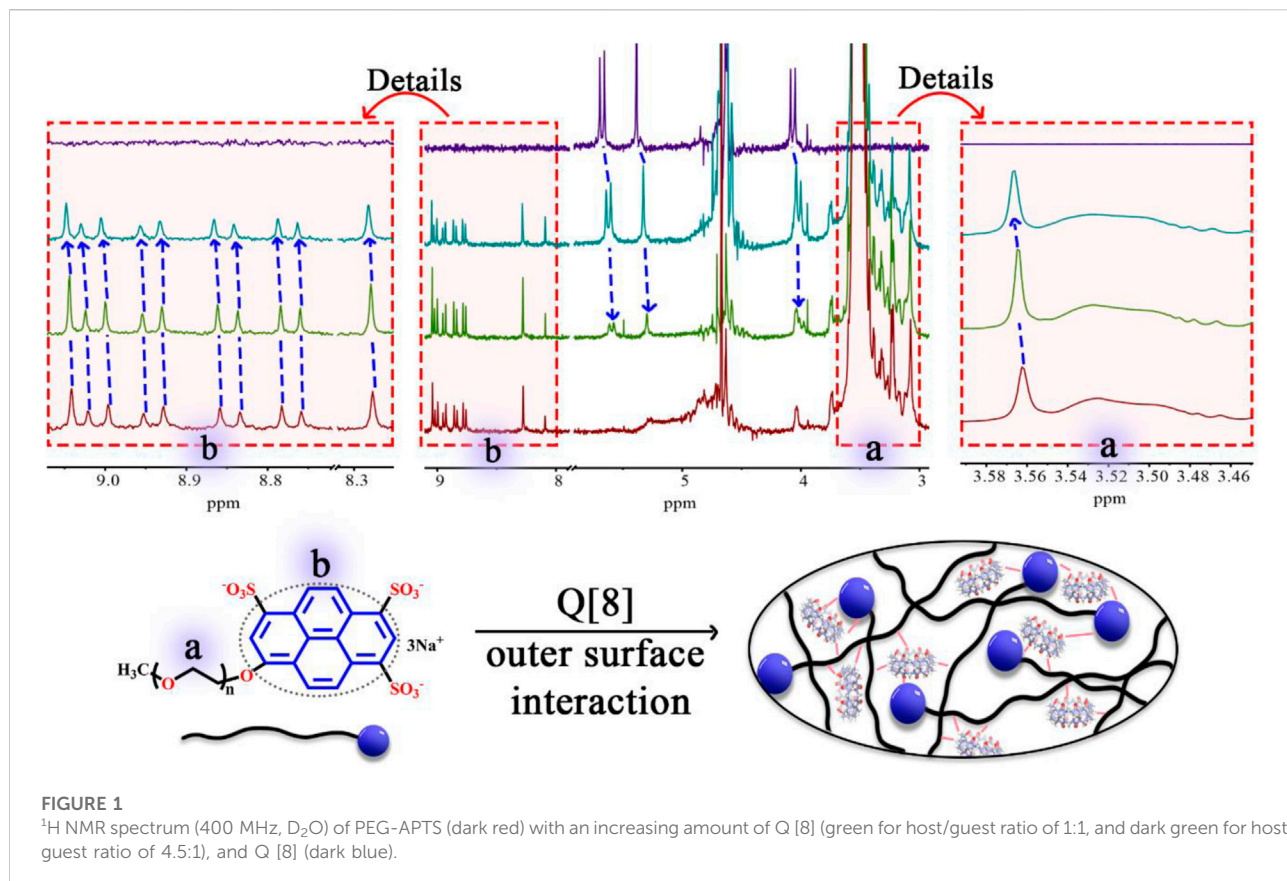
Results and discussion

Preparation and characterization of Q [8]@PEG-APTS

Based on the abundant hydrogen bonding sites, such as $\text{-SO}_3\text{H}$ functionalities and oxygen atoms, and the negative charge on PEG-APTS, fabrication of the stable supramolecular

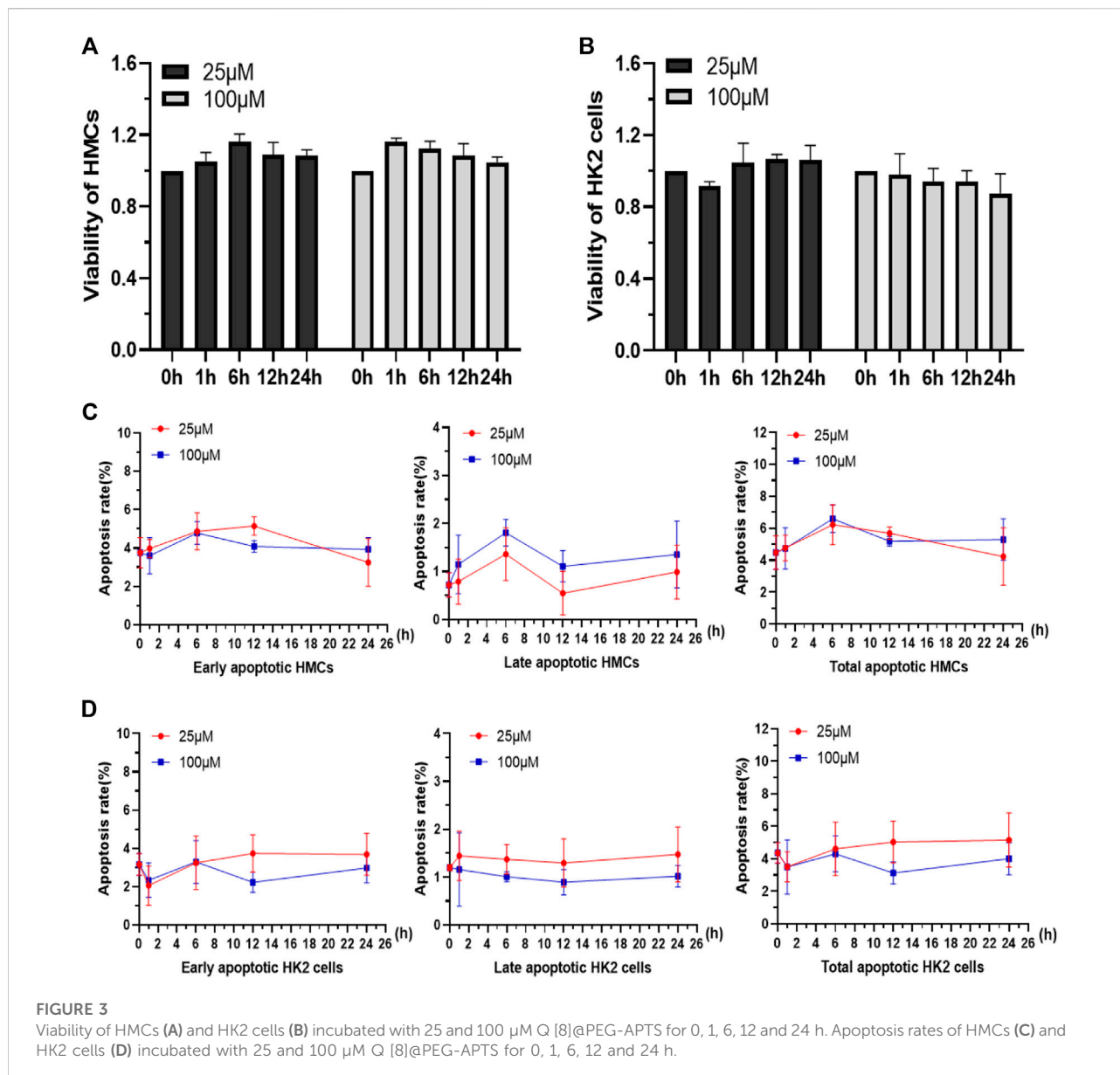
fluorescent materials can be achieved from PEG-APTS through the outer surface interaction of Q [8]. ^1H NMR titration, one of the most important tools to study supramolecular assembly, was carried out. From Figure 1, intensities of ^1H NMR peaks of both alkoxy chain and pyrene group of PEG-APTS shifted downfield after the addition of Q [8], which inferred the interaction of these protons with the deshielding effect of the outer surface of Q [8]. On contrary, the proton signal of Q [8] appeared at the more upfield position because of the altered microenvironment of the outer surface. This series of changes in the proton signal revealed powerful interactions within PEG-APTS and Q [8]. These interactions arrived from the abundant hydrogen bonding between oxygen atom in the alkoxy chain and the exposed methine on the outer surface of Q [8], C-H $\cdots\pi$ interaction of pyrene molecule with methine, $\pi\cdots\pi$ interaction of pyrene and carbonyl oxygen, and electrostatic interaction within $\text{-SO}_3\text{H}$ and the outer surface of Q [8]. Such rich interactions greatly improved the stability of supramolecular fluorescent materials, thereby providing the basis for subsequent studies.

In addition to ^1H NMR spectroscopy, both UV and fluorescence titration, the most common methods used understanding for supramolecular assemblies, were studied. As



shown in **Figure 2A**, the absorption of PEG-APTS gradually increased with increasing Q [8] concentration because that the outer surface interaction of Q [8] and PEG-APTS may induce the strong $n-\pi^*$ and $\pi-\pi^*$ interactions. From the fluorescence

titration, it was also observed that the addition of Q [8] slightly weakened the fluorescence performance of PEG-APTS, which indicated the elevated ACQ effect of fluorescent pyrene because the outer surface interaction, thereby improving the

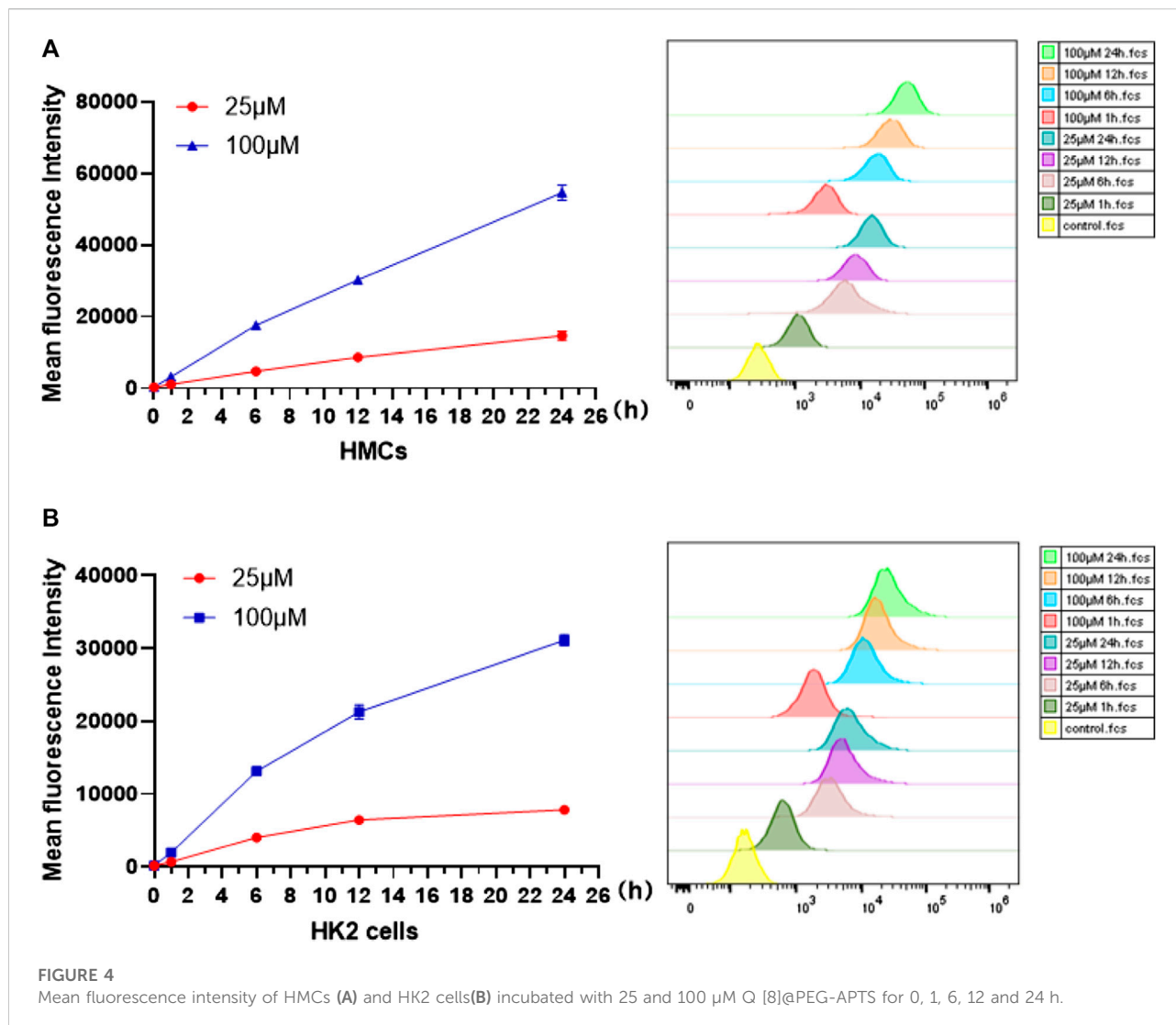


performance of supramolecular fluorescent materials disguisedly. To further characterize the morphology and size of supramolecular fluorescent material, DLS and SEM analyses were carried out.

From DLS results (Supplementary Figure S4), particle sizes of Q [8] (7.63 nm) and PEG-APTS (65.46 nm) were found to be relatively smaller than that of Q [8]@PEG-APTS (1149.93 nm), inferring the formation of Q [8]@PEG-APTS. From the SEM photomicrograph of Q [8]@PEG-APTS (Supplementary Figure S5), the supramolecular fluorescent material was observed to contain a regular, flattened ellipsoid surface.

Cytotoxicity studies of Q [8]@PEG-APTS in cells

Because of the aforementioned properties, the as-synthesized macromolecule was investigated to be used as a tool for kidney live cell tracing and drug detection *in vivo*. Herein, some preliminary works were carried out to investigate the application of Q [8]@PEG-APTS for tracing kidney live resident cells, such as HMC and HK2. The kidney is considered one of the most important metabolically active organs that consisted of several resident cells, such as mesangial cells, proximal tubular epithelial cells (PTECs), podocytes, and many more. Of these, mesangial cells provide



structural support for capillary loops and produce components of the glomerular matrix, (Kikkawa et al., 2003; Schlöndorff and Banas, 2009; Shotorbani et al., 2020; Avraham et al., 2021) whereas PTECs regulate the acid-base balance and body fluids homeostasis through reabsorption and secretion of electrolytes/metabolites (Nigam et al., 2015). From Figures 3A,B, HMCs and HK2 cells treated with 25 μM or 100 μM Q [8]@PEG-APTS exhibited no significant differences in relative viabilities among 0, 1, 6, 12, and 24 h groups. It was found that the viability rates of HMCs and HK2 cells cultured with Q [8]@PEG-APTS reached up to 85% under prolonged exposure to high concentrations (100 μM, 24 h). In addition, the early-, late-, and total-stage cellular apoptosis rates were not statistically different from the stimulation group, in which culture time was even up to 24 h for both cells. This has inferred that Q [8]@PEG-APTS possess low cytotoxicity towards HMCs and HK2 cells and therefore, can

further be applied for cell imaging and *in vivo* studies (Figures 3C,D).

Fluorescence imaging of Q [8]@PEG-APTS in cells

Before cell imaging, changes in fluorescence intensity in presence of Q [8]@PEG-APTS assemblies were investigated initially by using cell flowmetry. From Figure 4A,B, the mean fluorescence intensity (MIF) of Q [8]@PEG-APTS absorbed by HMCs and HK2 cells was found to increase gradually with the increase in incubation time and concentration to reach the maxima at 24 h with 100 μM. Moreover, the significantly increased fluorescence signals of Q [8]@PEG-APTS were observed in cells incubated with 25 μM for 1 h compared to

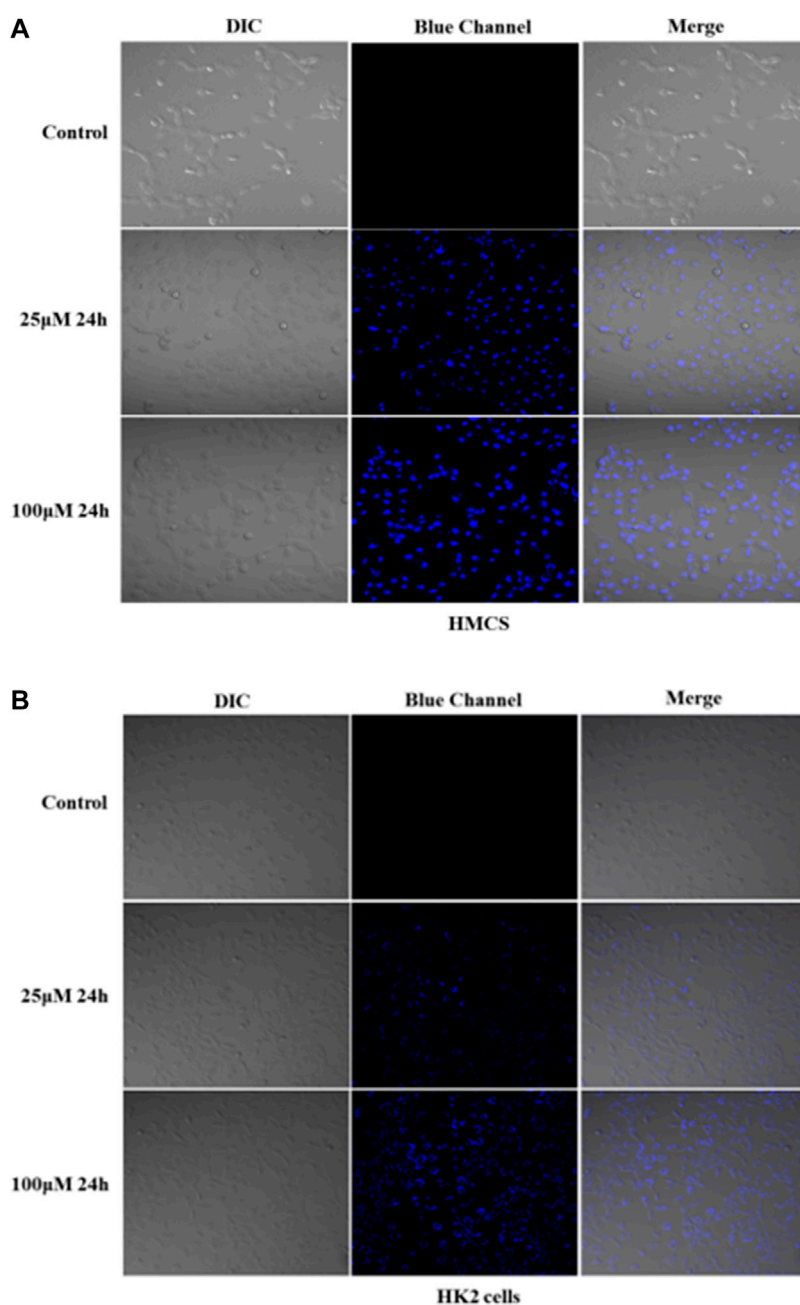


FIGURE 5

Confocal images of live HMCs (A) and HK2 cells (B) incubated with 25 and 100 μM Q [8]@PEG-APTS for 24 h (more details can be seen in [Supplementary Figures S7, S8](#)). Blue channel: $\lambda_{\text{ex}} = 405 \text{ nm}$, $\lambda_{\text{em}} = 450 \text{ nm}$. DIC, differential interference contrast in transmitted light images.

the control group ([Figure 4A,B](#)). The above results indicate that Q [8]@PEG-APTS assemblies were able to accumulate within the kidney cells in a relatively short period and reach the maxima at 24 h, possessing a very good kidney cell filtration capacity and the ability to be stable in cells and accumulate continuously.

Because of the good absorption for cells, Q [8]@PEG-APTS may be a potential biochemical tool to achieve *in vivo* cell imaging. Moreover, interestingly, uneven distribution

patterns of Q [8]@PEG-APTS within HMCs and HK2 cells were observed. Blue fluorescence dots clustered around the perinuclear of HMCs were observed while diffused over the entire cytoplasm in HK2 cells, and cells exhibited elevated fluorescence intensity with the increase in culture concentration ([Figure 5](#), [Supplementary Figures S7, S8](#)). In this context, Rajdeep Chowdhury et al. found that the fluorescent probe, 8-hydroxy-pyrene-1,3,6-trisulfonate

(HPTS), could be predominantly localized in the lysosome of lung cancer cells (Chowdhury et al., 2015). However, other researchers observed HPTS diffused in the cytosol of HeLa cells and Chinese hamster ovary cells (Sen Mojumdar et al., 2013; Cao et al., 2021). Therefore, the different distribution of Q [8]@PEG-APTS in these two types of renal residual cells has been the prime novelty of this study and this property may be helpful to identify diverse cell types when tracing live cells in the kidney. However, there are still many foundations works to apply Q [8]@PEG-APTS for the detection and diagnosis of kidney disease in clinical.

Experimental

Materials; instruments; and advanced characterization techniques, such as ¹H NMR, FT-IR, fluorescence spectrum, etc., are detailed in the supporting information. The detailed synthesis of PEG-APTS (Supplementary Scheme S2) is detailed in the supporting information. Herein, PEG-Cl (4 g, 2 mmol), 8-hydroxy-1,3,6-pyrene trisodium (1.048 g, 2 mmol), and 8.28 g anhydrous K₂CO₃ were added to 150 ml anhydrous DMF, followed by heating and refluxing at 130°C for 48 h. In the end, the solvent was removed by vacuum evaporation to obtain 2.8 g of brick-red solid crude product, of which 1.6 g of a brick-red solid product was obtained after purification by column chromatography using methanol as eluent. Detailed characterizations are given in the supporting information.

Conclusion

In this study, supramolecular fluorescent biomaterials Q [8]@PEG-APTS have been constructed by using synthesized polymers PEG-APTS and Q [8] through outer surface interaction. The biomaterials have been confirmed to possess a stable and uniform structure with brilliant fluorescence properties. Most importantly, the introduction of the positive density on the outer surface of Q [8]@PEG-APTS has made it faster to go through the glomerular filtration barrier and enter the kidney resident cells. Subsequently, this biomaterial has been able to accumulate selectively in the cytoplasm and nucleus of HK2 and HMCs cells, respectively, within 24 h, indicating that Q [8]@PEG-APTS may help in identifying different cell types when tracking live cells in the kidney. Follow-up, studies on the different recognition mechanisms of Q [8]@PEG-APTS in tracking live kidney cells are important to facilitate the simultaneous imaging and identification of mixed kidney cells, which is more suitable for early and rapid diagnosis of AKI, providing a theoretical basis for the potential application of Q [n]-based biomaterials in kidney research and therapy.

Data availability statement

The original contributions presented in the study are included in the article/Supplementary Material, further inquiries can be directed to the corresponding authors.

Author contributions

All authors made substantial contributions. QL and H-PY conceived and directed the project. HX and XY performed testing fluorescence property, biological toxicity and writing of the manuscript. LY helped in confocal imaging of cells. XX designed the chemical compound. DY and YL synthesized and tested the basic properties of the Q [8]@PEG-APTS. ZT participated in writing of the manuscript.

Funding

We thank the National Natural Science Foundation of China (NSFC no. 81970618 and 82170720), Science and Technology Research Project of Chongqing Education Commission (Grant no. KJZD-M201900401), Program for Youth Innovation in Future Medicine, Chongqing Medical University (no. W0098) and the Innovation Program for High-level Talents of Guizhou Province (no. 20165657) are gratefully acknowledged for financial support.

Conflict of interest

The authors declare that the research was conducted in the absence of any commercial or financial relationships that could be construed as a potential conflict of interest.

Publisher's note

All claims expressed in this article are solely those of the authors and do not necessarily represent those of their affiliated organizations, or those of the publisher, the editors and the reviewers. Any product that may be evaluated in this article, or claim that may be made by its manufacturer, is not guaranteed or endorsed by the publisher.

Supplementary material

The Supplementary Material for this article can be found online at: <https://www.frontiersin.org/articles/10.3389/fchem.2022.974607/full#supplementary-material>

References

- Assaf, K. I., and Nau, W. M. (2015). Cucurbiturils: From synthesis to high-affinity binding and catalysis. *Chem. Soc. Rev.* 44, 394–418. doi:10.1039/c4cs00273c
- Avraham, S., Korin, B., Chung, J. J., Oxburgh, L., and Shaw, A. S. (2021). The Mesangial cell - the glomerular stromal cell. *Nat. Rev. Nephrol.* 17, 855–864. doi:10.1038/s41581-021-00474-8
- Barrow, S. J., Kasera, S., Rowland, M. J., del Barrio, J., and Scherman, O. A. (2015). Cucurbituril-based molecular recognition. *Chem. Rev.* 115, 12320–12406. doi:10.1021/acs.chemrev.5b00341
- Basile, D. P., Bonventre, J. V., Mehta, R., Nangaku, M., Unwin, R., Rosner, M. H., et al. (2016). Progression after AKI: Understanding maladaptive repair processes to predict and identify therapeutic treatments. *J. Am. Soc. Nephrol.* 27, 687–697. doi:10.1681/asn.2015030309
- Cao, J., Xie, M., Gao, X., Zhang, Z., Wang, J., Zhou, W., et al. (2021). Charge neutralization strategy to construct salt-tolerant and cell-permeable nanoprobes: Application in ratiometric sensing and imaging of intracellular pH. *Anal. Chem.* 93, 15159–15166. doi:10.1021/acs.analchem.1c03629
- Chawla, L. S., Eggers, P. W., Star, R. A., and Kimmel, P. L. (2014). Acute kidney injury and chronic kidney disease as interconnected syndromes. *N. Engl. J. Med.* 371, 58–66. doi:10.1056/NEJMra1214243
- Chen, J., Li, S. K., Wang, Z. Y., Pan, Y. T., Wei, J. W., Lu, S. Y., et al. (2021). Synthesis of an AIEgen functionalized cucurbit[7]uril for subcellular bioimaging and synergistic photodynamic therapy and supramolecular chemotherapy. *Chem. Sci.* 12, 7727–7734. doi:10.1039/d1sc01139a
- Cheng, X. J., Liang, L. L., Chen, K., Ji, N. N., Xiao, X., Zhang, J. X., et al. (2013). Twisted cucurbit[14]uril. *Angew. Chem. Int. Ed.* 52, 7252–7255. doi:10.1002/anie.201210267
- Chowdhury, R., Saha, A., Mandal, A. K., Jana, B., Ghosh, S., and Bhattacharyya, K. (2015). Excited state proton transfer in the lysosome of live lung cells: Normal and cancer cells. *J. Phys. Chem. B* 119, 2149–2156. doi:10.1021/jp503804y
- Cui, L., Vivona, S., Smith, B. R., Kothapalli, S. R., Liu, J., Ma, X., et al. (2020). Reduction triggered *in situ* polymerization in living mice. *J. Am. Chem. Soc.* 142, 15575–15584. doi:10.1021/jacs.0c07594
- Fisch, S., Liao, R., Hsiao, L. L., and Lu, T. (2016). Early detection of drug-induced renal hemodynamic dysfunction using sonographic technology in rats. *J. Vis. Exp.* 109, e52409. doi:10.3791/52409
- Goldstein, S. L., Mottes, T., Simpson, K., Barclay, C., Muething, S., Haslam, D. B., et al. (2016). A sustained quality improvement program reduces nephrotoxic medication-associated acute kidney injury. *Kidney Int.* 90, 212–221. doi:10.1016/j.kint.2016.03.031
- Jia, J., Wen, H., Zhao, S., Wang, L., Qiao, H., Shen, H., et al. (2019). Displacement induced Off-On fluorescent biosensor targeting Ido1 activity in live cells. *Anal. Chem.* 91, 14943–14950. doi:10.1021/acs.analchem.9b03387
- Kao, C. C., Yang, W. S., Fang, J. T., Liu, K. D., and Wu, V. C. (2019). Remote organ failure in acute kidney injury. *J. Formos. Med. Assoc.* 118, 859–866. doi:10.1016/j.jfma.2018.04.005
- Kellum, J. A., Romagnani, P., Ashuntantang, G., Ronco, C., Zarbock, A., and Anders, H. J. (2021). Acute kidney injury. *Nat. Rev. Dis. Prim.* 7, 52–68. doi:10.1038/s41572-021-00284-z
- Kikkawa, Y., Virtanen, I., and Miner, J. H. (2003). Mesangial cells organize the glomerular capillaries by adhering to the G domain of laminin $\alpha 5$ in the glomerular basement membrane. *J. Cell Biol.* 161, 187–196. doi:10.1083/jcb.200211121
- Kim, J., Jung, I. S., Kim, S. Y., Lee, E., Kang, J. K., Sakamoto, S., et al. (2000). New cucurbituril homologues: syntheses, isolation, characterization, and X-ray crystal structures of cucurbit[n]uril (n = 5, 7, and 8). *J. Am. Chem. Soc.* 122, 540–541. doi:10.1021/ja993376p
- Kobayashi, H., Kawamoto, S., Jo, S. K., Sato, N., Saga, T., Hiraga, A., et al. (2002). Renal tubular damage detected by dynamic micro-MRI with a dendrimer-based magnetic resonance contrast agent. *Kidney Int.* 61, 1980–1985. doi:10.1046/j.1523-1755.2002.00364.x
- Lerman, L. O., Rodriguez-Porcel, M., and Romero, J. C. (1999). The development of x-ray imaging to study renal function. *Kidney Int.* 55, 400–416. doi:10.1046/j.1523-1755.1999.00301.x
- Li, Y., Dong, Y., Miao, X., Ren, Y., Zhang, B., Wang, P., et al. (2018). Shape-controllable and fluorescent supramolecular organic frameworks through aqueous host-guest complexation. *Angew. Chem. Int. Ed. Engl.* 130, 737–741. doi:10.1002/ange.201710553
- Lin, R. L., Liu, J. X., Chen, K., and Redshaw, C. (2020). Supramolecular chemistry of substituted cucurbit[n]urils. *Inorg. Chem. Front.* 7, 3217–3246. doi:10.1039/d0qi00529k
- Liu, J., Lan, Y., Yu, Z., Tan, C. S. Y., Parker, R. M., Abell, C., et al. (2017). Cucurbit[n]uril-Based microcapsules self-assembled within microfluidic droplets: A versatile approach for supramolecular architectures and materials. *Acc. Chem. Res.* 50, 208–217. doi:10.1021/acs.accounts.6b00429
- Liu, M., Chen, L., Shan, P., Lian, C., Zhang, Z., Zhang, Y., et al. (2021). Pyridine detection using supramolecular organic frameworks incorporating cucurbit [10] uril. *ACS Appl. Mat. Interfaces* 13, 7434–7442. doi:10.1021/acsami.0c20292
- Liu, Z., Krishna, S., Nalluri, M., and Stoddart, J. F. (2017). Surveying macrocyclic chemistry: From flexible crown ethers to rigid cyclophanes. *Chem. Soc. Rev.* 46, 2459–2478. doi:10.1039/c7cs00185a
- Luo, Y., Zhang, W., Yang, M. X., Feng, X. H., Redshaw, C., Li, Q., et al. (2022b). A twisted cucurbit[14]uril-based fluorescent supramolecular polymer mediated by metal ion. *Macromolecules* 55 (5), 1642–1646. doi:10.1021/acs.macromol.2c00075
- Luo, Y., Gan, S. Q., Zhang, W., Jia, M. H., Chen, L. X., Redshaw, C., et al. (2022a). A new cucurbit[10]uril-based AIE fluorescent supramolecular polymer for cellular imaging. *Mat. Chem. Front.* 6, 1021–1025. doi:10.1039/d2qm00084a
- Mei, J., Leung, N. L. C., Kwok, R. T. K., Lam, J. W. Y., and Tang, B. Z. (2015). Aggregation-induced emission: together we shine, united we soar. *Chem. Rev.* 115, 11718–11940. doi:10.1021/acs.chemrev.5b00263
- Moore, C., Borum, R. M., Mantri, Y., Xu, M., Fajtová, P., O'Donoghue, A. J., et al. (2021). Activatable carbocyanine dimers for photoacoustic and fluorescent detection of protease activity. *ACS Sens.* 6, 2356–2365. doi:10.1021/acssensors.1c00518
- Murray, J., Kim, K., Ogoshi, T., Yao, W., and Gibb, B. C. (2017). The aqueous supramolecular chemistry of cucurbit[n]urils, pillar[n]-arenes and deep-cavity cavitands. *Chem. Soc. Rev.* 46, 2479–2496. doi:10.1039/c7cs00095b
- Ni, X. L., Xiao, X., Cong, H., Zhu, Q. J., Xue, S. F., and Tao, Z. (2014). Self-assemblies based on the “outer-surface interactions” of cucurbit[n]urils: New opportunities for supramolecular architectures and materials. *Acc. Chem. Res.* 47, 1386–1395. doi:10.1021/ar5000133
- Nigam, S. K., Wu, W., Bush, K. T., Hoening, M. P., Blantz, R. C., and Bhatnagar, V. (2015). Handling of drugs, metabolites, and uremic toxins by kidney proximal tubule drug transporters. *Clin. J. Am. Soc. Nephrol.* 10, 2039–2049. doi:10.2215/cjn.02440314
- Palivan, C. G., Goers, R., Najer, A., Zhang, X., Car, A., and Meier, W. (2016). Bioinspired polymer vesicles and membranes for biological and medical applications. *Chem. Soc. Rev.* 45, 377–411. doi:10.1039/c5cs00569h
- Pazhayattil, G. S., and Shirali, A. C. (2014). Drug-induced impairment of renal function. *Int. J. Nephrol. Renov. Dis.* 7, 457–468. doi:10.2147/ijnr.d.s39747
- Peerapornratana, S., Manrique-Caballero, C. L., Gomez, H., and Kellum, J. A. (2019). Acute kidney injury from sepsis: Current concepts, epidemiology, pathophysiology, prevention and treatment. *Kidney Int.* 96, 1083–1099. doi:10.1016/j.kint.2019.05.026
- Sato, R., Luthe, S. K., and Nasu, M. (2017). Blood pressure and acute kidney injury. *Crit. Care* 21, 28. doi:10.1186/s13054-017-1611-7
- Schlöndorff, D., and Banas, B. (2009). The mesangial cell revisited: No cell is an island. *J. Am. Soc. Nephrol.* 20, 1179–1187. doi:10.1681/asn.2008050549
- Sen Mojumdar, S., Chowdhury, R., Mandal, A. K., and Bhattacharyya, K. (2013). What time scale proton transfer takes place in a live CHO cell. *J. Chem. Phys.* 138, 215102. doi:10.1063/1.4807862
- Shotorbani, P. Y., Chaudhari, S., Tao, Y., Tsiokas, L., and Ma, R. (2020). Inhibitor of myogenic differentiation family isoform a, a new positive regulator of fibronectin production by glomerular mesangial cells. *Am. J. Physiology-Renal Physiology* 318, F673–F682. doi:10.1152/ajprenal.00508.2019
- Wang, L., Xu, M., Zhou, H., Yan, K., Duan, S., Xue, D., et al. (2022). Teaching PCR for simultaneous sensing of gene transcription and downstream metabolites by cucurbit[8]uril-mediated intervention of polymerase activity. *Anal. Chem.* 94, 8715–8723. doi:10.1021/acs.analchem.2c01103
- Wu, L., Huang, J., Pu, K., and James, T. D. (2021). Dual-locked spectroscopic probes for sensing and therapy. *Nat. Rev. Chem.* 5, 406–421. doi:10.1038/s41570-021-00277-2
- Yang, D., Liu, M., Xiao, X., Tao, Z., and Redshaw, C. (2021). Polymeric self-assembled cucurbit[n]urils: Synthesis, structures and applications. *Coord. Chem. Rev.* 434, 213733. doi:10.1016/j.ccr.2020.213733
- Zhang, W., Luo, Y., Zhao, J., Lin, W. H., Ni, X. L., Tao, Z., et al. (2022a). tQ[14]-based AIE supramolecular network polymers as potential bioimaging agents for the detection of Fe³⁺ in live HeLa cells. *Sensors Actuators B Chem.* 354, 131189. doi:10.1016/j.snb.2021.131189
- Zhang, W., Luo, Y., Yang, M. X., Li, W. H., Redshaw, C., Ni, X. L., et al. (2022c). Twisted cucurbit[14]uril: A new type of CTE macrocycle for Fe sensing. *Microchem. J.* 178, 107364. doi:10.1016/j.microc.2022.107364
- Zhang, W., Luo, Y., Zhao, J., Zhang, C., Ni, X. L., Tao, Z., et al. (2022b). Controllable fabrication of a supramolecular polymer incorporating twisted cucurbit[14]uril and cucurbit[8]uril via self-sorting. *Chin. Chem. Lett.* 33, 2455–2458. doi:10.1016/j.ccl.2021.11.053
- Zhang, X. D., Chen, K., and Sun, W. Y. (2021). Potential applications of cucurbit [n]urils and their derivatives in the capture of hazardous chemicals. *Chem. Eur. J.* 27, 5107–5119. doi:10.1002/chem.202004711